Water Research 229 (2023) 119448

Contents lists available at ScienceDirect

Water Research

journal homepage: www.elsevier.com/locate/watres

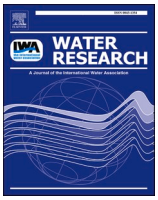

# Rainstorms drive export of aromatic and concurrent bio-labile organic matter to a large eutrophic lake and its major tributaries

Yongqiang Zhou [a,b,1,*], Xiaoqin Yu [a,1,2], Lei Zhou [c], Yunlin Zhang [a,b], Hai Xu [a,b], Mengyuan Zhu [a,b], Guangwei Zhu [a,b], Kyoung-Soon Jang [d], Robert G.M. Spencer [e], Erik Jeppesen [f,g,h,i], Justin D. Brookes [j], Dolly N Kothawala [k], Fengchang Wu [l]

[a] Taihu Laboratory for Lake Ecosystem Research, State Key Laboratory of Lake Science and Environment, Nanjing Institute of Geography and Limnology, Chinese Academy of Sciences, Nanjing 210008, China
[b] University of Chinese Academy of Sciences, Beijing 100049, China
[c] State Key Laboratory of Soil and Sustainable Agriculture, Institute of Soil Science, Chinese Academy of Sciences, 71 East Beijing Road, Nanjing 210008, China
[d] Bio-Chemical Analysis Group, Korea Basic Science Institute, Cheongju 28119, South Korea
[e] Department of Earth, Ocean and Atmospheric Science, Florida State University, Tallahassee, Florida 32306, United States
[f] Department of Ecoscience and Center for Water Technology (WATEC), Aarhus University, C.F. Møllers Allé 3, 8000 Aarhus, Denmark
[g] Sino–Danish Centre for Education and Research, Beijing 100190, China
[h] Limnology Laboratory, Department of Biological Sciences and Centre for Ecosystem Research and implementation, Middle East Technical University, Ankara 06800, Turkey
[i] Institute of Marine Sciences, Middle East Technical University, Mersin 33731, Turkey
[j] Water Research Centre, School of Biological Science, The University of Adelaide, 5005 Adelaide, Australia
[k] Department of Ecology and Genetics/Limnology, Uppsala University, Uppsala 75236, Sweden
[l] State Key Laboratory of Environmental Criteria and Risk Assessment, Chinese Research Academy of Environmental Sciences, Beijing 100012, China

ARTICLE INFO

*Keywords:*
Dissolved organic matter
Rainstorms
FT-ICR MS
Lake Taihu
Molecular composition

ABSTRACT

Lakes are hotspots for global carbon cycling, yet few studies have explored how rainstorms alter the flux, composition, and bio-lability of dissolved organic matter (DOM) in inflowing rivers using high-frequency monitoring. We conducted extensive campaigns in the watershed of Lake Taihu and made daily observations for three years in its two largest inflowing tributaries, River Dapu and River Yincun. We found higher DOC, bio-labile DOC (BDOC), and specific UV absorbance ($SUVA_{254}$) levels in the northwestern inflowing regions compared with the remaining lake regions. DOC and BDOC increased during rainstorms in River Dapu, and DOC declined due to local dilution and BDOC increased during rainstorms in River Yincun. We found that rainstorms resulted in increased DOM absorbance $a_{350}$, $SUVA_{254}$, and humification index (HIX) and enhanced percentages of humic-like fluorescent components, %polycyclic condensed aromatic and %polyphenolic compounds as revealed from ultrahigh-resolution mass spectrometry (FT-ICR MS), while spectral slope ($S_{275\text{-}295}$) and the percentages of protein-like C1 and C3 declined during rainstorms compared with other seasons. This can be explained by a combined flushing of catchment soil organic matter and household effluents. The annual inflows of DOC and BDOC to Lake Taihu were $1.15 \pm 0.18 \times 10^4$ t C $yr^{-1}$ and $0.23 \pm 0.06 \times 10^4$ t C $yr^{-1}$ from River Dapu and $2.92 \pm 0.42 \times 10^3$ t C $yr^{-1}$ and $0.53 \pm 0.07 \times 10^3$ t C $yr^{-1}$ from River Yincun, respectively, and the fluxes of DOC and BDOC from both rivers increased during rainstorms. We found an elevated frequency of heavy rainfall and rainstorms in the lake watershed during the past six decades. We conclude that an elevated input of terrestrial organic-rich DOM with concurrent high aromaticity and high bio-lability from inflowing rivers is likely to occur in a future wetter climate.

* Corresponding author.
*E-mail address:* yqzhou@niglas.ac.cn (Y. Zhou).
[1] Y. Zhou and X. Yu contributed equally to this work.
[2] Present address: Luoshe Senior High School, Wuxi 214000, China.

https://doi.org/10.1016/j.watres.2022.119448
Received 6 September 2022; Received in revised form 29 November 2022; Accepted 30 November 2022
Available online 1 December 2022

## 1. Introduction

Terrestrial landscapes have been estimated to deliver up of 5.1 Pg C $yr^{-1}$ to inland waters, including lakes and rivers, of which approximately 3.9 Pg C $yr^{-1}$ is outgassed as $CO_2$ (Drake et al., 2018). Dissolved organic matter (DOM) in fluvial environments are primarily derived from leaching of soil organic matter and flushing of organic substances from impervious land cover in terrestrial landscapes (Hosen et al., 2014; Zhou et al., 2022). The quantity, timing, and chemical composition of DOM exported to rivers and downstream-linked lakes are largely constrained by land use, topography, and hydrology (Drake et al., 2019; Johnston et al., 2020; Zhou et al., 2022). Lakes and reservoirs are typically the most important sources of water for large and mega cities. Lake DOM is of special concern for drinking water treatment as DOM may interfere with the drinking water treatment processes, and is expensive to remove (Baghoth et al., 2011; Tomlinson et al., 2016). DOM can be responsible for unpleasant odor and taste, formation of carcinogenic disinfection by-products, and toxicity and bio-availability of micropollutants (Stedmon et al., 2011; Kothawala et al., 2017). The reactivity and fate of DOM are closely associated with its chemical composition (Kellerman et al., 2015), and the hydrological connectivity of upstream landscapes largely controls the chemical composition of DOM in the downstream receiving waters (Lynch et al., 2019; Johnston et al., 2020; Zhou et al., 2020).

Traditional approaches for quantifying riverine carbon fluxes often rely on periodical sampling at weekly, monthly, or even seasonal temporal resolution, but this often fails to capture the biogeochemical changes in DOM composition during episodical storm events (Hur et al., 2014; Spencer et al., 2016). Rainstorm events are a major driver that pulses the export of terrestrial DOM and carbon-bound nutrients into streams, rivers, and downstream-linked lake ecosystems. Rainfall has been shown to be responsible for 86% of the annual dissolved organic carbon (DOC) export with large rainfalls contributing to 57% of the DOC exported in 30 small forested watersheds in the eastern USA (Raymond and Saiers, 2010). An extreme five-day rainstorm event during the passage of Hurricane Irene resulted in the export of 43% of the annual DOC and 31% of the annual dissolved organic nitrogen fluxes in Esopus Creek in New York (Yoon and Raymond, 2012). Despite the importance of rainstorm events in influencing the export of DOC, only a few studies to-date have explored the DOC flux during rainstorm events (Yoon and Raymond, 2012; Zhou et al., 2020). Long-term high-frequency field observations, especially campaigns conducted during the occurrence of rainstorm events, can help elaborate advanced management schemes for large lakes (Zhou et al., 2020). However, it remains unclear how rainstorms alter the flux, chemical composition, and bio-lability of DOM exported to large eutrophic lakes.

A recent study carried out in a mountainous valley in southern China indicated that the occurrence and intensity of heavy rainfall, with rainfall intensity $\geq$ 25 mm $d^{-1}$ and rainstorms with rainfall intensity $\geq$ 50 mm $d^{-1}$ have increased during the past six decades (Zhou et al., 2020). Other recent studies conducted in the Lake Taihu watershed indicate that the net discharge of inflowing stream water is more relevant to DOM composition than catchment area with urban land use or population density (Zhou et al., 2018a; Zhou et al., 2018b). It remains unclear to what extent the frequency and intensity of heavy rainfall and rainstorm events will increase specifically in the Yangtze River Delta, which is one of the most developed regions in China. It is also unclear if rainstorms will pulse the export of terrestrial DOM and nutrients to lakes, fueling further eutrophication of these waters.

The aim of this study is to quantify how rainstorm events impact the flux, chemical composition, and bio-lability of DOM exported to large, shallow, and hyper-eutrophic Lake Taihu via its major inflowing tributaries. We carried out an extensive field sampling campaign across the lake ($n$ = 35) and its surrounding rivers ($n$ = 209) during the wet-to-dry transition season and took daily measurements at the two largest inflowing tributaries, River Dapu and River Yincun, for almost three year, from January 1, 2019 to December 8, 2021 ($n$ = 1,073). We hypothesized that during extreme rainstorm events, the mobilization of soil organic matter and flushing of non-point source DOM over impervious landscapes in densely populated areas would result in elevated export of both aromatic soil organic matter and aliphatic energy-rich DOM contributing to higher bio-lability.

## 2. Materials and methods

### 2.1. Study area

Lake Taihu is the third largest freshwater lake in China. It is located in the Yangtze River Delta and has a surface area of 2,338 $km^2$ and a mean depth of 1.9 m (Fig. S1). According to the Taihu Basin hydrological information service system (http://www.tba.gov.cn/), the lake watershed can be divided into seven sub-watersheds: Huxi, Wuchengxiyu, Yangchengdianmao, Hangjiahu, Zhexi, Pudong, and Puxi (Fig. S1c). A total of 172 rivers or channels are connected to the lake, and most of these channels have water levels lower than 5 m.a.s.l. (Qin et al., 2019). Most of the inflowing tributaries are situated in the western and northern part of the lake watershed, while the main outflow rivers are mainly found in the southeastern watershed. River Dapu and River Yincun are the two largest inflowing tributaries, both draining the northwestern densely populated Huxi sub-watershed. River Yincun has a mean population density of ~670 $km^{-2}$ and had a mean gross domestic product (GDP) of 6900 $\times$ $10^4$ RMB $km^{-2}$ in 2015 with well-developed fisheries in the upstream region. In comparison, River Dapu had a mean population density of ~530 $km^{-2}$ and a mean GDP of 5400 $\times$ $10^4$ RMB $km^{-2}$ in 2015, with high cropland coverage in the upstream catchment. Data on land use (urban + agricultural land use), gross domestic product (GDP), and population density of the seven sub-watersheds obtained from the Resource and Environment Science and Data Center (https://www.resdc.cn/) are in Table S2 of Supporting Information.

### 2.2. Sample collection and hydrological data collection

A total of 1,314 water samples were collected from the lake and connecting rivers and channels. This sample set consisted of 1,073 samples taken daily from the two largest inflowing tributaries draining into the northwestern part of Lake Taihu, River Dapu and River Yincun, over almost three years, from January 1, 2019 to December 8, 2021 (see red stars on Fig. S1 for the location of sampling sites). Another subset of 241 samples were collected from the rivers and channels connecting to the lake ($n$ = 209; white triangles on Fig. S1) and the lake itself ($n$ = 32; white circles on Fig. S1) in May 2021. The extensive spatial sampling campaigns were carried out in May (rainy-to-dry transition season) and were designed serve as a baseline for DOM composition across the lake and tributaries and excludes disturbances from rainstorms or the long-term dry season. Surface (0.5 m) water samples were collected using acid-cleaned plastic bottles, and stored in the field in a cool box under dark conditions. The samples were transported to the laboratory for filtration immediately following sampling campaigns, and DOM optical measurements were completed within three days of sampling. Long-term (2015-2020) seasonal variability in total nitrogen (TN) and total phosphorus (TP) concentrations are found in the Supporting Information.

Data on the daily water levels of River Dapu and River Yincun and estimated inflow discharge from January 2019 to December 2021 (data on inflow discharge not available as from March 2021) from the two largest inflowing rivers were obtained from the Taihu Basin hydrological information service system (http://www.tbhi.gov.cn//tba/content/SWJ/sqyb/index.html). Long-term daily rainfall data (from January 1, 1959 to December 31, 2021) recorded at the four meteorological gauging stations – Dongshan, Wuxi, Yixing, and Huzhou – surrounding Lake Taihu were obtained from the China Meteorological Data Sharing

Service System (http://data.cma.cn/). Heavy rainfall and rainstorm events were defined as rainfall intensity ≥ 25 mm $d^{-1}$ and ≥ 50 mm $d^{-1}$, respectively (Zhou et al., 2020).

### 2.3. Measurements of DOC, bioavailable DOC (BDOC), and DOM absorption

Water samples were filtered through pre-combusted Whatman GF/F filters (0.7 μm) and analyzed for dissolved organic carbon (DOC) concentration using a total organic carbon analyzer (TOC-VCPN, Shimadzu, Tokyo, Japan) at high temperature (680 °C) after acidification with 10 μL 85% $H_3PO_4$. Biodegradable DOC (BDOC) was measured as the fraction of DOC degraded by microbes over a 28 days of dark incubation (Vonk et al., 2015). Detailed information on bio-incubation experiments can be found in the Supporting Information. Water samples were re-filtered through 0.7 μm filters after 28 days of bio-incubation prior to DOC measurements to remove the interference of flocculation and production of particulate organic carbon during the bio-incubation. Percent BDOC (%BDOC) was calculated from the ratio of DOC consumed vs the initial DOC concentration during the 28 days of laboratory bio-incubation (Abbott et al., 2014; Vonk et al., 2015).

Subsequently, the water samples were filtered through pre-rinsed Millipore membrane cellulose filters (0.22 μm) to determine DOM absorbance and fluorescence excitation-emission matrices (EEMs). DOM absorbance spectra between 200 and 800 nm at 1 nm intervals were obtained using a Shimadzu UV-2550PC UV-Vis spectrophotometer with matching 5 cm quartz cells. Calibration of DOM optical spectra can be found in the Supporting Information. In this study, the absorption coefficient at 350 nm, $a_{350}$, was used as a surrogate for chromophoric DOM. The specific ultraviolet DOM absorbance at 254 nm, i.e. $SUVA_{254}$, was calculated as DOM absorbance at 254 nm normalized to DOC concentration, and $SUVA_{254}$ is a surrogate indicator of DOM aromaticity (Weishaar et al., 2003). DOM spectral slope ($S_{275\text{-}295}$) was calculated by a nonlinear fit over the 275-295 nm range and is expected to increase with a decreasing terrestrial soil organic matter inputs (Helms et al., 2008; Cédric and Benner 2012).

### 2.4. DOM fluorescence measurements and PARAFAC modeling

DOM fluorescence excitation-emission matrices (EEMs) were measured with an F-7000 fluorescence spectrometer (Hitachi High Technologies, Tokyo, Japan) equipped with a 700-voltage xenon lamp at room temperature (20 ± 2 °C). Detailed EEM calibration procedures can be found in the Supporting Information and briefly daily DOM fluorescence was calibrated to the water Raman peak area, with results normalized to Raman unit (R.U.) (Stedmon et al., 2011). The humification index (HIX) was used to characterize the degree of humification of DOM (Huguet et al., 2009).

PARAFAC modeling was conducted with drEEM toolbox (ver. 0.2.0) in MATLAB R2015b (Murphy et al., 2013) with details in the Supporting Information. The spectral shapes of the four identified PARAFAC components were compared with those identified earlier in other aquatic ecosystems using an online spectral library called OpenFluor (Murphy et al., 2014). C1 ($E_x/E_m$ = 275/316 nm) was similar to those of tyrosine-like substances (Kothawala et al., 2014; Margaret et al., 2016) (Fig. S2). C2 ($E_x/E_m$ = 255/452 nm) can be categorized as a terrestrial humic-like substance (Walker et al., 2013; Sankar et al., 2019) (Fig. S2). C3 ($E_x/E_m$ = 235/340 nm) displayed spectral shapes congruent with amino-acid-associated tryptophan-like components (Stedmon and Markager 2005; Yamashita et al., 2013) (Fig. S2). C4 ($E_x/E_m$ = 245 (270)/388 nm) was characterized as a microbial humic-like fluorophore and supposedly microbial humic-like acid produced from algae and bacteria (Stedmon and Markager 2005; Murphy et al., 2011) (Fig. S2).

### 2.5. Fourier transform ion cyclotron resonance mass spectrometry (FT-ICR MS) and data processing

A total of ten water samples collected from River Dapu, the largest inflowing river to the lake, across gradients of rainfall intensity and water level were solid-phase extracted using 3 mL PPL Bond Elut (Agilent) resins according to the method described elsewhere (Zhou et al., 2020) to investigate how rainstorm changes the molecular composition of DOM. Briefly, 20-30 mL water samples (volumes were adjusted depending on DOC concentration to ensure extraction of similar loads of DOC, i.e. 60 μgC) were filtered through 0.22 μm filters and acidified to pH = 2 with 10 M HCl. The samples were slowly passed through PPL cartridges (~ 5 mL $min^{-1}$), and 6 mL of 0.01 M HCl were filtered through the cartridges before these were dried with pure $N_2$ gas. DOM samples together with a Milli-Q blank sample were eluted using 1 mL methanol. The final extracts were diluted 1:1 with Milli-Q water and analyzed using a 15 Tesla FT-ICR MS via negative ion mode with electrospray ionization at the Korea Basic Science Institute, Ochang, Korea (Choi et al., 2019). The data accuracy was within an error of < 0.3 ppm after internal calibration using Data Analysis Software version 3.4, Bruker Daltonik GmbH (Fu et al., 2020).

The modified aromaticity index ($AI_{mod}$) was calculated, and $AI_{mod}$ increased with increasing aromaticity of DOM (Koch and Dittmar 2006; Koch and Dittmar 2016). Using O/C and H/C molar ratios exhibited in van Krevelen diagrams together with $AI_{mod}$, DOM was categorized into: 1) polycyclic condensed aromatics ($AI_{mod}$ > 0.66), 2) polyphenolic compounds (0.5 < $AI_{mod}$ ≤ 0.66), 3) highly unsaturated phenolic compounds ($AI_{mod}$ < 0.5 and H/C < 1.5), 4) aliphatics (1.5 ≤ H/C < 2 and N = 0), 5) peptide-like compounds (1.5 ≤ H/C < 2 and N > 0), and 6) sugar-like compounds (H/C ≥1.5 and O/C > 0.9) (Spencer et al., 2014; Coward et al., 2019; Kellerman et al., 2019).

### 2.6. Statistical analyses

The spatial distribution of sampling sites and DOM-related parameters were mapped using ArcGIS 10.2, and PARAFAC modeling was performed using the drEEM toolbox with MATLAB R2019b. Statistical analyses, including mean values, standard deviations (SD), linear regressions, and Wilcoxon tests, were conducted using R x64 4.0.5 and MATLAB 2019b software. Significance values of $p < 0.05$ were reported for Wilcoxon tests and linear regressions.

## 3. Results

### 3.1. Variations in DOM quality in the lake and its tributaries

In Lake Taihu, DOC ranged from 2.5 to 5.7 mg·$L^{-1}$ with a mean of 3.9 ± 0.5 mg·$L^{-1}$ (mean ± SD, here and thereafter). We found higher DOC, TN and TP levels in the northwestern inflowing lake regions compared with other areas in all seasons (Fig. 1a; Fig. S3-Fig. S4), and the mean DOC level was significantly higher in the surrounding rivers (5.28 ± 1.61 mg·$L^{-1}$) than in the lake (Wilcoxon test, $p < 0.001$). BDOC in the surrounding river samples (28 ± 11%) was significantly higher than that of the lake samples (21 ± 5%, Wilcoxon test, $p < 0.001$) (Fig. S3b), and greatest in the weastern part of the lake (Fig. 1b). $SUVA_{254}$ levels and contribution of terrestrial humic-like %C2 were higher in the northwestern inflowing tributaries (Fig. 1c-d; Fig. S3c-d).

### 3.2. Daily observations from the largest tributaries River Yincun and River Dapu

During the daily observations from January 1, 2019 to December 8, 2021, the mean water level of River Dapu (3.45 ± 0.33 m) was slightly lower than in River Yincun (3.57 ± 0.31 m) and followed highly comparable temporal patterns (Fig. 2a). The peak water levels of these two large rivers, River Yincun and River Dapu, occurred in August of all

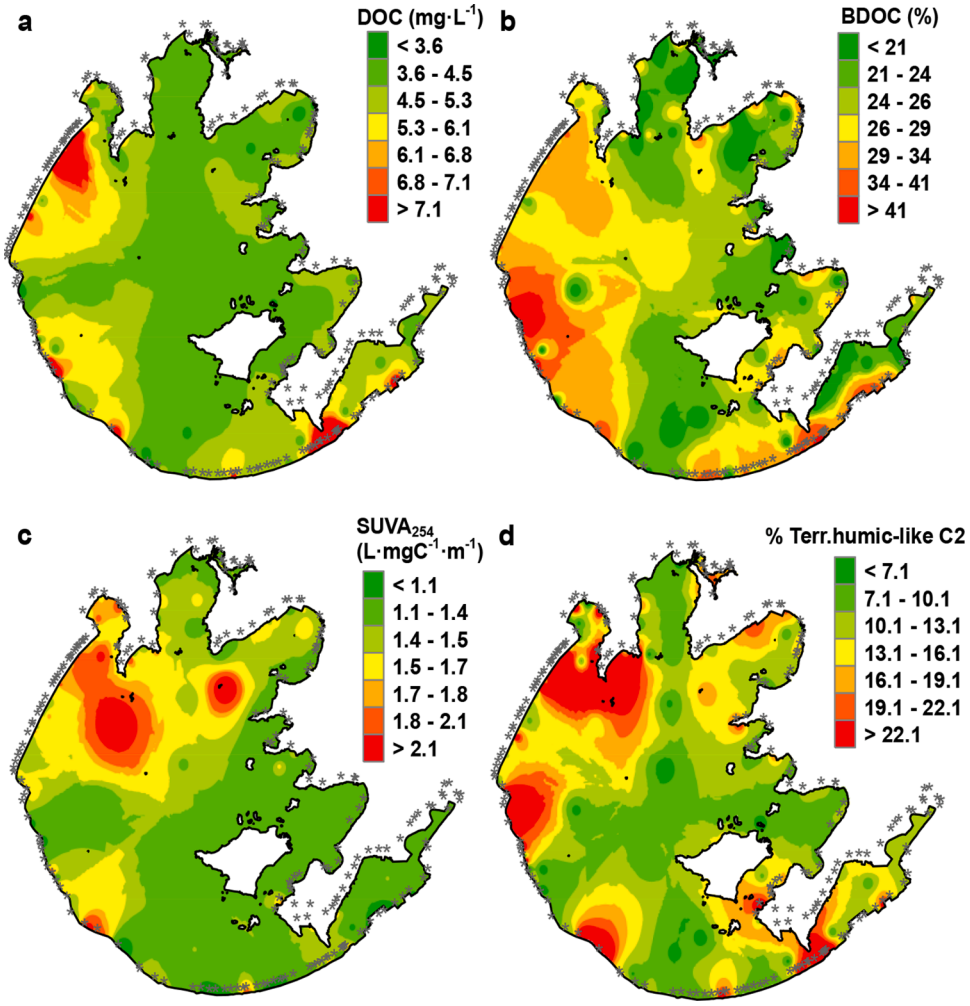


**Fig. 1.** Spatial variability of (a) dissolved organic carbon (DOC) concentration, (b) percent bio-degradable organic carbon (BDOC), (c) specific UV absorbance ($SUVA_{254}$), and (d) the contribution of terrestrial humic-like C2 (in %) in Lake Taihu and the surrounding rivers in May 2021. Samples were collected in May, i.e. wet-to-dry transition season, to avoid interference of rainstorm-induced floods or long-term low lake water levels. Points denote the location of a total of 209 riverine sampling sites.

years. A total of eleven rainstorm events ($\geq$ 50 mm $d^{-1}$) were recorded in the three-year daily observations (marked in gray, Fig. 2a). The mean DOC concentration of River Dapu (4.26 $\pm$ 0.62 mg·$L^{-1}$) was significantly higher than in River Yincun (4.03 $\pm$ 0.72 mg·$L^{-1}$) (paired Wilcoxon test, $p < 0.001$; Fig. 2b). BDOC of the two rivers ranged from 0.2% to 57%, and the mean BDOC of River Dapu was 23 $\pm$ 12%, which was significantly higher than in River Yincun (19 $\pm$ 10%) (paired Wilcoxon test, $p < 0.01$; Fig. 2c). Multiplying daily DOC and BDOC levels with the daily mean inflow discharge from the two rivers, we estimated the mean annual inflow of DOC to Lake Taihu to be 1.15 $\pm$ 0.18 $\times$ $10^4$ t C $yr^{-1}$ from River Dapu and 2.92 $\pm$ 0.42 $\times$ $10^3$ t C $yr^{-1}$ from River Yincun, while the annual BDOC inflows were 0.23 $\pm$ 0.06 $\times$ $10^4$ t C $yr^{-1}$ from River Dapu and 0.53 $\pm$ 0.07 $\times$ $10^3$ t C $yr^{-1}$ from River Yincun over 2019-2021. We further estimated that during rainstorms, the DOC flux ranged from 34.0 to 62.3 t $d^{-1}$ and the BDOC flux from 10.3 to 25.5 t $d^{-1}$ in River Dapu, while the DOC flux ranged from 11.3 to 18.2 t $d^{-1}$ and the BDOC flux from 3.1 to 4.6 t $d^{-1}$ in River Yincun, being much higher during rainstorms than in the low water periods.

### 3.3. Relationships between water level and DOM-related indices in River Dapu and River Yincun

When the water level of the two rivers were lower than 3.8 m.a.s.l. (below flood warning water levels of both rivers), DOC increased with increasing water level in both River Dapu ($r^2 = 0.09$, $p < 0.001$) and River Yincun ($r^2 = 0.08$, $p < 0.001$), and BDOC increased with increasing water level in River Dapu ($r^2 = 0.11$, $p < 0.001$) and River Yincun ($r^2 = 0.09$, $p < 0.001$) (Fig. 2d-e). In contrast, when the water level of the two rivers was higher than 3.8 m.a.s.l. (above flood warning water levels), DOC decreased with increasing water level in River Dapu ($r^2 = 0.34$, $p < 0.001$) and River Yincun ($r^2 = 0.06$, $p < 0.01$), and BDOC decreased with increasing water level in River Dapu ($r^2 = 0.47$, $p < 0.01$) and River Yincun ($r^2 = 0.61$, $p < 0.001$) (Fig. 2f-g).

During the whole three-year observation period, we found that $a_{350}$ ($p < 0.001$), $SUVA_{254}$ ($p < 0.001$), HIX ($p < 0.001$), terrestrial humic-like %C2 ($p < 0.001$), and microbial humic-like %C4 ($p < 0.001$) increased with increasing water levels in both River Dapu and River Yincun (Fig. 3; Fig. 4). In comparison, $S_{275\text{-}295}$ ($p < 0.001$), tyrosine protein-like %C1 ($p < 0.001$), and tryptophan protein-like %C3 ($p < 0.001$) decreased with increasing daily water levels for both rivers (Fig. 3; Fig. 4).

### 3.4. Comparison of DOC, BDOC and optical metric between rainstorm and sunny conditions

To explore the impact of rainstorm events relative to rain free periods, we compared the mean DOC, BDOC, and optical indices during rainstorm events (indicated in grey in in Fig. 2a-c) with those during sunny days. DOC and BDOC increased from 4.2 $\pm$ 0.8 mg·$L^{-1}$ and 21.5% $\pm$ 15.0% during sunny days to 4.7 $\pm$ 1.1 mg·$L^{-1}$ and 31.2 $\pm$ 13.0% during rainstorm events in River Dapu (Wilcoxon test, $p < 0.001$; Fig. 5a-b) and from 4.2 $\pm$ 0.8 mg·$L^{-1}$ and 20.2% $\pm$ 14.1% during sunny days to 3.8 $\pm$ 0.4 mg·$L^{-1}$ and 27.1% $\pm$ 7.6% during rainstorm events in River Yincun (Wilcoxon test, $p < 0.001$; Fig. 5a-b). $SUVA_{254}$ of the two rivers increased from 2.0 $\pm$ 0.5 L·mg $C^{-1}$·$m^{-1}$ during sunny days to 2.3 $\pm$ 0.5

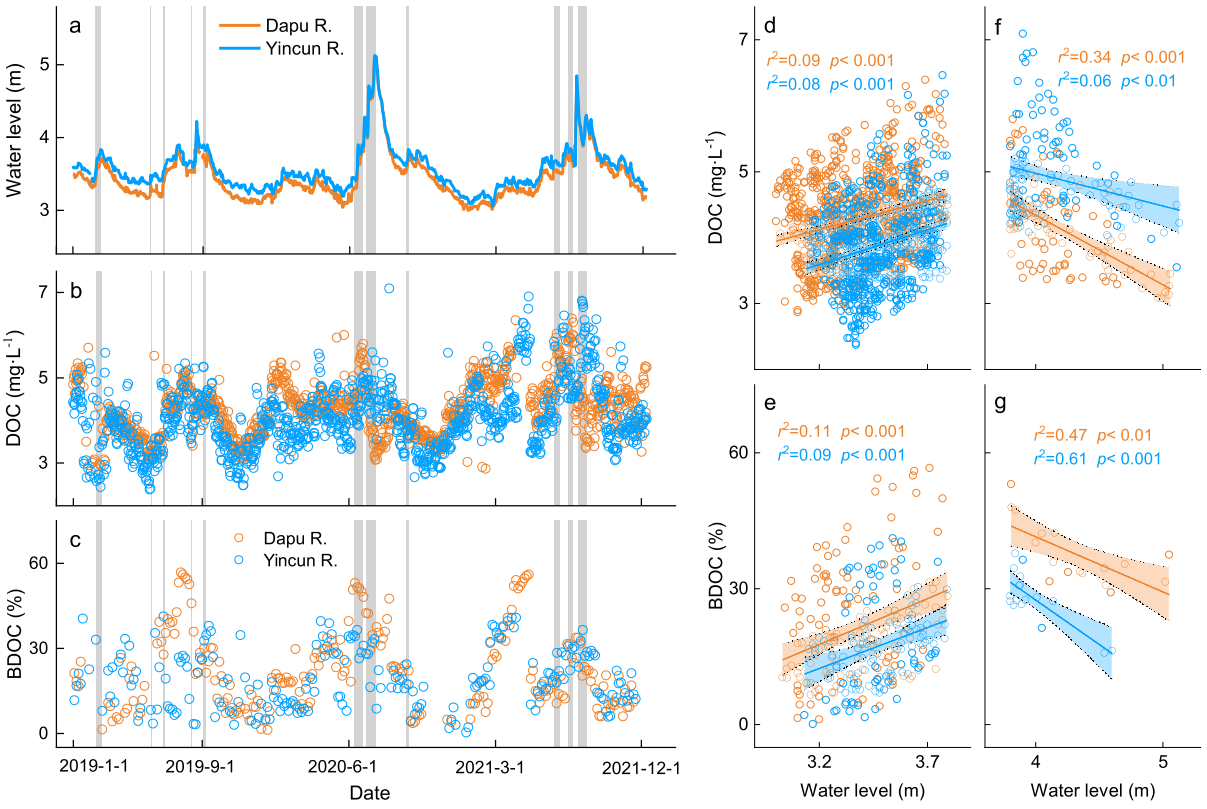


**Fig. 2.** (a) Daily water level at the two gauging stations Chengdonggang of River Dapu and Wuxiqiao of River Yincun running into Lake Taihu. (b) Dissolved organic carbon (DOC) of the samples collected daily from January 1, 2019 to December 8, 2021 in River Dapu and River Yincun. (c) Bio-labile DOC (BDOC) of the samples collected every three days day from January 1, 2019 to December 8, 2021 in River Dapu and River Yincun. The gray regions in panels a-c denote the occurrence and persistence of rainstorm events. (d-e) Relationships between water level and DOC (d), BDOC (e) when the water levels of both River Dapu and River Yincun were lower than 3.8 m.a.s.l. (below flood warning water level of both rivers) with typical long-term sunny days. Relationships between water level and DOC (f), BDOC (g) when the water levels of both rivers were both higher than 3.8 m.a.s.l. (above flood warning water level) with typical long-term rainfall.

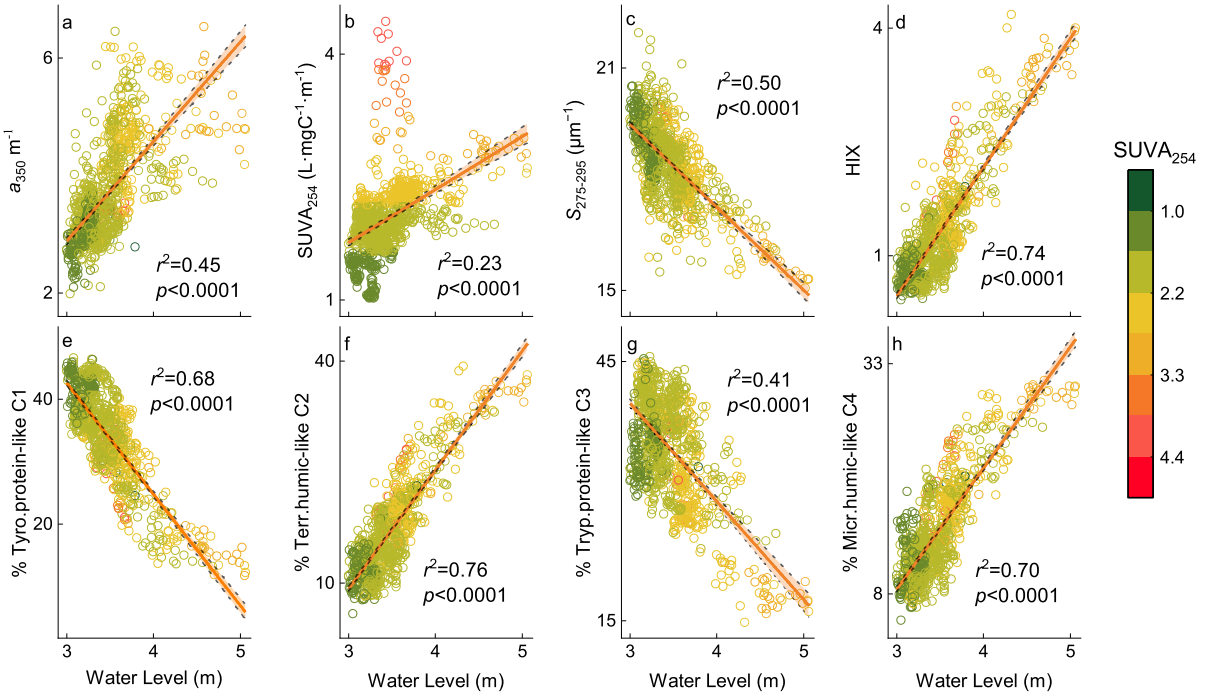


**Fig. 3.** Relationships between the water level during the day preceding the samplings and (a) DOM absorbance, $a_{350}$ ($m^{-1}$), (b) specific ultraviolet absorbance at 254 nm ($SUVA_{254}$) ($L{\cdot}mgC^{-1}{\cdot}m^{-1}$), (c) spectral slope ($S_{275\text{-}295}$) ($\mu m^{-1}$), (d) humification index (HIX), and (e-h) contribution percentage of the four PARAFAC components %C1-C4 (%) for the samples collected from River Dapu from January 1, 2019 to December 8, 2021.

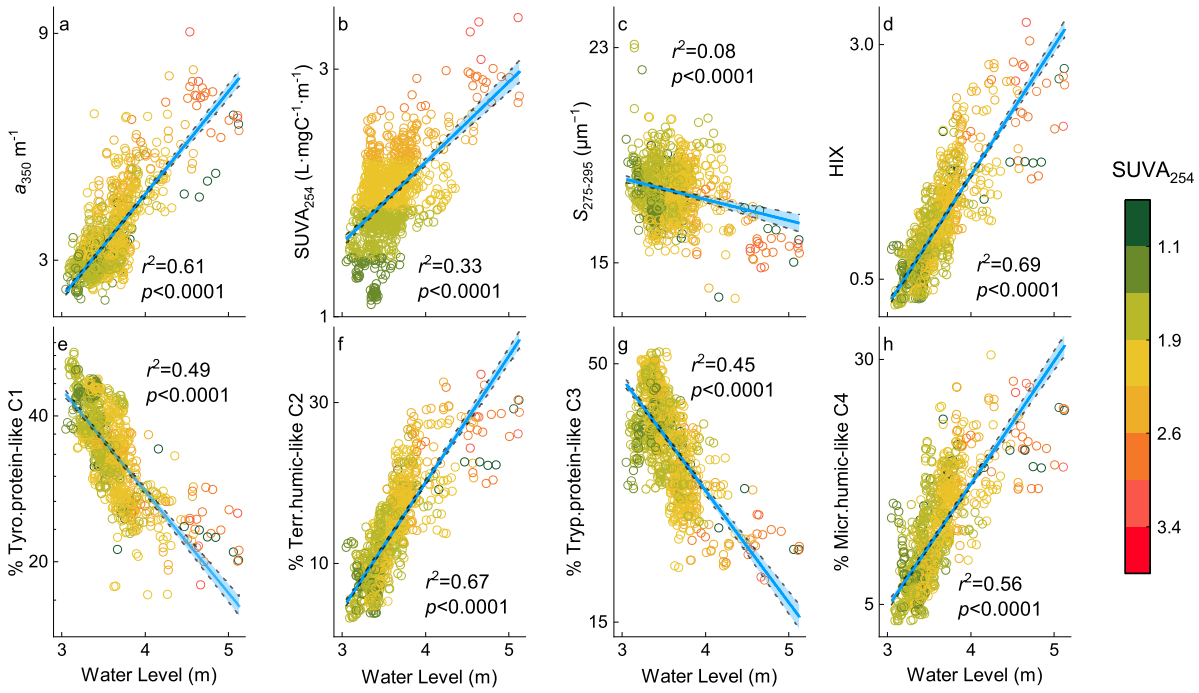


**Fig. 4.** Relationships between the water level during the day preceding the samplings and (a) DOM absorbance, $a_{350}$ (m$^{-1}$), (b) specific ultraviolet absorbance at 254 nm (SUVA$_{254}$) (L·mgC$^{-1}$·m$^{-1}$), (c) spectral slope ($S_{275\text{-}295}$) (μm$^{-1}$), (d) humification index (HIX), and (e-h) contribution percentages of the four PARAFAC components %C1-C4 (%) for the samples collected from River Yincun from January 1, 2019 to December 8, 2021.

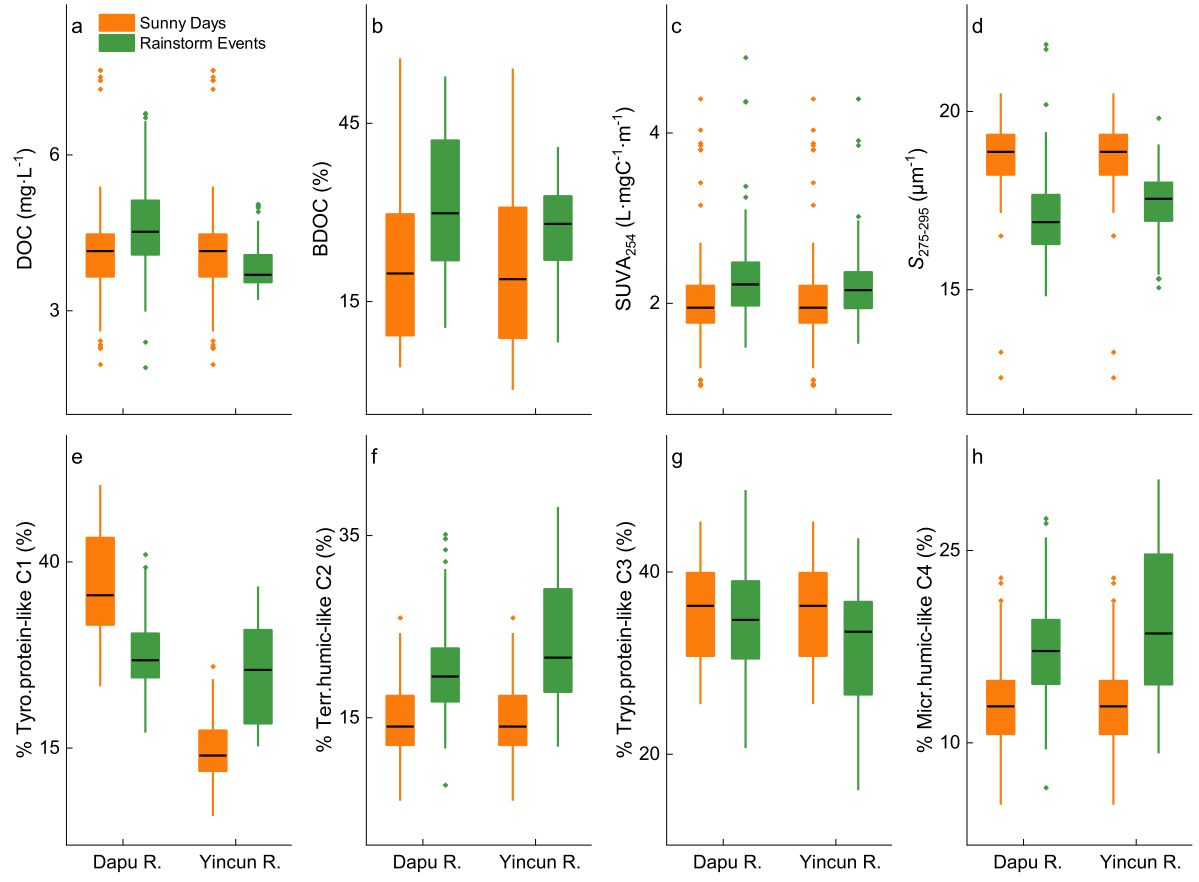


**Fig. 5.** Comparison of DOM-related parameters of the samples taken from River Dapu and River Yincun during sunny days and rainstorm events shown in Fig. 2, respectively. DOM-related parameters include the concentrations of dissolved organic carbon (DOC; mg·L$^{-1}$) (a), bio-degradable DOC (BDOC; %) (b), specific ultraviolet absorbance at 254 nm, SUVA$_{254}$ (L·mg·C$^{-1}$·m$^{-1}$) (c), spectral slope, $S_{275\text{-}295}$ (μm$^{-1}$) (d), contribution percentages of tyrosine-like C1 (%) (e), terrestrial humic-like C2 (%) (f), tryptophan-like C3 (%) (g), and microbial humic-like C4 (%) (h).

L·mg $C^{-1}$·$m^{-1}$ during rainstorms (Wilcoxon test, $p < 0.001$; Fig. 5), $S_{275-295}$ decreased from 18.8 ± 0.9 $\mu m^{-1}$ during sunny days to 17.2 ± 1.2 $\mu m^{-1}$ during rainstorms (Wilcoxon test, $p < 0.001$), tyrosine-like %C1 decreased from 36.6% ± 6.6% to 26.4% ± 5.8% (Wilcoxon test, $p < 0.001$), terrestrial humic-like C2 increased from 14.8% ± 3.8% to 21.9% ± 6.5% (Wilcoxon test, $p < 0.001$; Fig. 5), tryptophan-like %C3 decreased from 35.5% ± 5.1% to 32.9% ± 7.0% (Wilcoxon test, $p < 0.001$; Fig. 5), and microbial humic-like %C4 increased from 13.1% ± 7.2% to 18.7% ± 5.3% (Wilcoxon test, $p < 0.001$; Fig. 5).

### 3.5. Principal component analysis (PCA) results

We used principal component analysis (PCA) to investigate the impacts of rainstorms on the chemical composition of DOM samples taken from River Dapu and River Yincun. As for the River Dapu samples, the first two principal components, PC1 and PC2, explained 68.3% and 10.6%, respectively, of all the variables included (Fig. 6). In comparison, for the samples collected from River Yincun, PC1 and PC2 explained 68.5% and 11.1%, respectively. For both rivers, we found that $S_{275-295}$, %C1, and %C3 showed positive PC1 loadings, whereas the daily water level, $a_{350}$, $SUVA_{254}$, HIX, %C2, and %C4 exhibited negative loadings (Fig. 6). $S_{275-295}$ is typically negatively associated with the terrestrial input of DOM (i.e., increasing aromaticity) (Helms et al., 2008), C1 and C3 can be categorized into protein-like components, and $SUVA_{254}$ and HIX are positively associated with the aromaticity of DOM, implying that PC1 was negatively associated with the relative contribution of terrestrial aromatic DOM and positively with the autochthonous production of protein-like substances. We found that PC1 scores decreased significantly with the increasing water levels in both rivers ($p < 0.0001$) (Fig. 6).

### 3.6. FT-ICR MS results from River Dapu at contrasting water levels

The mean ratio of mass to charge ($m/z$) was lower (mean $m/z \sim 349.3$) for the samples collected in the low water level season of River Dapu (3.55 m) than in the high water level season (5.05 m) with a mean $m/z \sim 363.3$ (Fig. 7a). In general, there was an enrichment of formulae with lower H/C (< 1.5) during high water level period (Fig. 7b). Meanwhile, the relative abundance-weight contributions (%RA) of polycyclic and condensed aromatic and polyphenolic compounds increased during high discharge events, corresponding to depleted %RA of the highly unsaturated and phenolic and aliphatic compounds (Fig. 7b; Table S1). Spearman's rank order correlation analysis revealed that the relative abundance of polycyclic and condensed aromatic and polyphenolic compounds increased with an increasing percentage of terrestrial humic-like C2 and water level (rho > 0.5, $p < 0.05$), while the relative abundance of the highly unsaturated and phenolic and aliphatic compounds decreased with an increasing percentage of terrestrial humic-like C2 and water level (rho > 0.5, $p < 0.05$) (Fig. 7c-d). The percentage of terrestrial humic-like C2 increased, while the %RA of H/C ratio of DOM decreased significantly with increasing water levels (Fig. 7e-f; Table S1).

### 3.7. Long-term (1959–2021) trends of heavy rain and rainstorm events

According to the historical rainfall monitoring data (1959-2021) of the meteorological gauging stations of Dongshan, Wuxi, Yixing, and Huzhou surrounding Lake Taihu, an occurrence frequencies of both heavy rainfall (≥ 25 mm $d^{-1}$) and rainstorm (≥ 50 mm $d^{-1}$) events were recorded (Fig. 8). Enhanced intensity of heavy rainfall events but not of rainstorm events was recorded from 1959 to 2021. Based on the simple linear regression models, we observed that the frequency of heavy rainfall increased from 11 times per year in 1959 to 14 times per year in 2021, and rainstorm events increased from ~twice per year in 1959 to ~3 times per year in 2021 (Fig. 8). The mean intensity of heavy rainfall in the lake catchment increased from 34.0 ± 3.7 mm $d^{-1}$ in 1959 to 41.2 ± 1.4 mm $d^{-1}$ in 2021 (Fig. 8).

## 4. Discussion

Our extensive spatial and temporal sampling program coupled with long-term high-frequency field observations revealed that compared with low water seasons, rainstorm events resulted in increased DOC and BDOC levels and thereby rapid flushing and export of freshly mobilized terrestrial DOM with high bio-lability and concurrent high aromaticity to Lake Taihu via its two major inflowing tributaries.

The chemical composition of DOM in Lake Taihu was strongly influenced by the mobilization of terrestrial soil organic matter and non-point source effluents from the northwestern inflowing Huxi sub-watershed. Firstly, we found high levels of DOC in the northwestern inflowing Huxi sub-watershed and the northwestern lake regions, coinciding with the high levels of $SUVA_{254}$ and BDOC recorded here compared with the remaining sub-watersheds and also the remaining lake regions (Fig. 1; Fig. S3). This suggests that terrestrial input of aromatic organic-rich DOM is mainly derived from inflowing large rivers (including the two largest tributaries of the lake, i.e. River Dapu and

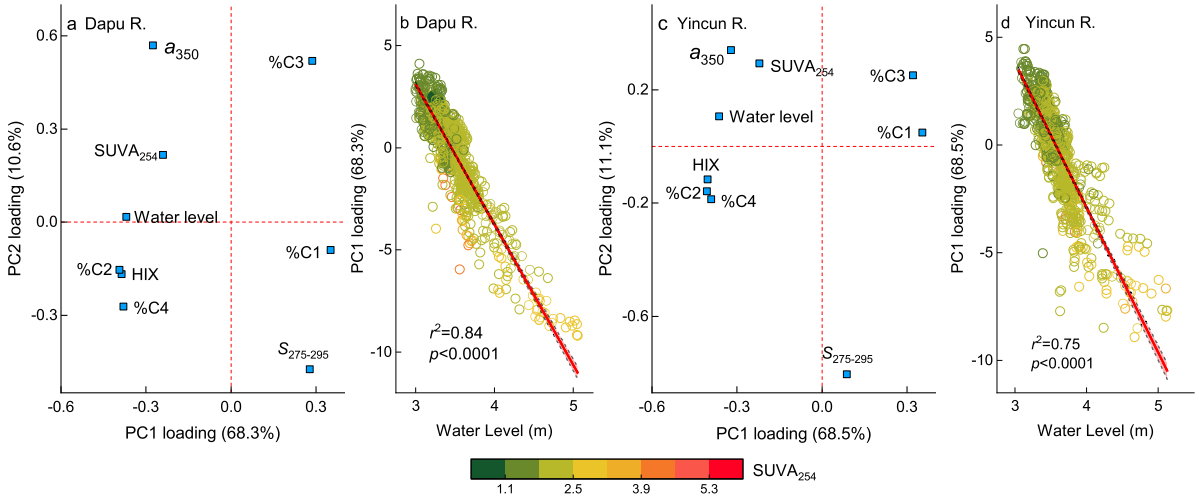


**Fig. 6.** Loadings of the first two axes of principal components analysis (PCA) encompassing the daily water level and DOM-related parameters, including DOM absorbance ($a_{350}$), specific UV absorbance ($SUVA_{254}$), spectral slope ($S_{275-295}$), humification index (HIX), and the contribution of the four PARAFAC components, i.e. %C1-%C4, and the relationships between PC1 scores and water level for the samples taken from River Dapu (a-b) and River Yincun (c-d).

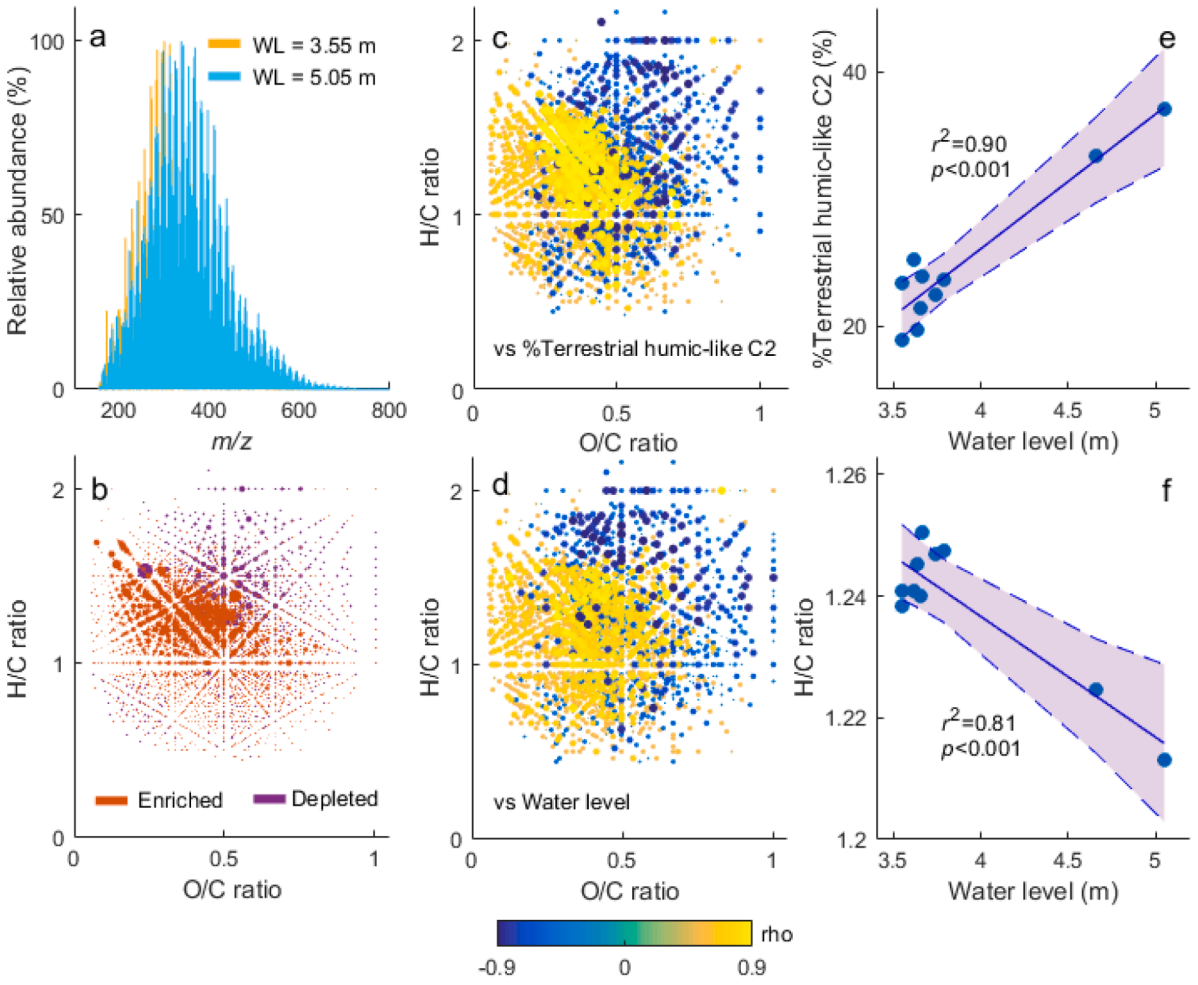


**Fig. 7.** Ultrahigh resolution mass spectra (FT-ICR MS) exhibiting the *m/z* range 150~800 for the samples collected from River Dapu with end member water level (WL) at 3.55 m and 5.05 m (a), and van Krevelen diagram showing the molecular formulae of enriched and depleted relative abundance at high water level (WL = 5.05) relative to that at low water level (WL = 3.55) (b). Spearman correlation coefficients (rho) between the relative abundance of molecular formulae for samples from River Dapu ($n$ = 10) and the contribution of terrestrial humic-like C2 (c) and water level (d), with only statistically significant results ($p < 0.05$) included. Relationships between the contribution of terrestrial humic-like C2, i.e. %C2 (%) (e), the relative abundance-weighted H/C ratio of the assigned formulae (f), and the water level of River Dapu.

River Yincun) in these regions. Previous studies suggested high terrestrial DOM inputs from northwestern sub-watersheds despite the relatively low disturbed land use and GDP here (Table S2), which coincided well with the high inflowing discharge from this region compared with the remaining areas (Zhou et al., 2018a; Zhou et al., 2018b). The lake has a short average water residence time (~300 d), and riverine DOM draining household sewage, fishery effluent, and terrestrial soil organic matter therefore contribute importantly to the DOM pool in the lake (Zhou et al., 2018a). Secondly, the significant positive relationships between daily water level and $a_{350}$, $SUVA_{254}$, $I_C$:$I_T$, HIX, %C2, and %C4 of the two rivers (Fig. 3; Fig. 4) were consistent with the findings of previous studies (Fasching et al., 2016), which indicates that terrestrial aromatic DOM increased with the increasing riverine water level as C2 is a typical terrestrial humic-rich component, and C4 is also closely associated with terrestrial soil organic matter inputs (Yamashita and Jaffé 2008). This is further supported by the elevated DOC in River Dapu but not River Yincun, and the elevated BDOC, DOM aromaticity, and percentages of humic-like C2 and C4 in both rivers during rainstorms (Fig. 5). The increased percentages of these two components during rainstorms with elevated water levels may be attributed to the enhanced mobilization of soil organic matter and terrestrial plant remnants. Rainstorm events result in an elevated flow path of surface runoff and groundwater flow from the deep organic-depleted mineral layer to the upper organic-rich and litter layer (Yang et al., 2015; Zhou et al., 2020), which may further enhance both the freshness and aromaticity of the exported DOM. Accordingly, we found a negative association between PC1 and DOM aromaticity with increasing water levels (Fig. 6). The elevated aromaticity of DOM during rainstorms may be explained by the inputs of rainwater humic-rich DOM during rainstorm events as rainwater DOM is closely associated with aromatic atmospheric dust and aerosols or aerosol-phase humic-like substances (Zhang et al., 2014; Zhou et al., 2017). The aromatic fraction of DOM has been suggested to be hydrophobic (Dilling and Kaiser 2002; Kothawala et al., 2014), and DOM aromaticity therefore increases with increasing removal efficiency during coagulation and associates closely with the formation potential of trihalomethane during disinfection (Edzwald and Tobiason 1999; Jung and Son 2008; Kothawala et al., 2017). Our results therefore highlight the importance of high-frequency monitoring when advising regarding the time of withdrawal of raw water for drinking water treatment (Zhou et al., 2020), and provides background information about the strong relationship between DOM composition and hydrology in a large shallow eutrophic urban lake.

We found elevated bio-degradability of DOM exported via the two rivers during rainstorms, which has important implications for $CO_2$ production and suggest storm water derived DOM provides an important energy source for higher trophic levels of the food web. This observation

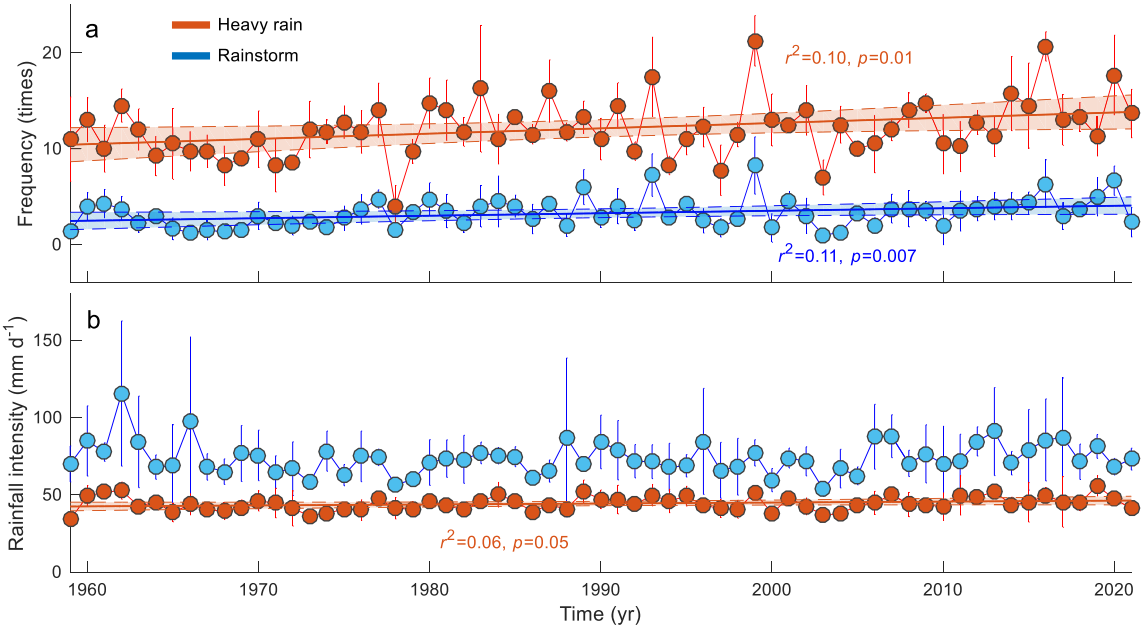


**Fig. 8.** Long-term trends in (a) the frequency and (b) rainfall intensity of heavy rainfall events (orange lines) and rainstorm events (blue lines) from 1959 to 2021 in the watershed of Lake Taihu. Error bars in panels a-b represent ±1 S.D. of the frequency and rainfall intensity of heavy rainfall (≥ 25 mm d$^{-1}$) and rainstorm events (≥ 50 mm d$^{-1}$) at the four metrological gauging stations Dongshan, Wuxi, Yixing, and Huzhou in the surrounding areas of the lake within the Lake Taihu watershed.

was supported by elevated BDOC in both rivers during rainstorm events compared with sunny days (Fig. 5) and also the significant negative relationships between the daily water level and $S_{275\text{-}295}$ in both rivers (Fig. 3; Fig. 4). BIX, %C1, and %C3 all decreased with increasing water level in both rivers (Fig. 3; Fig. 4), suggesting rapid flushing and dilution of household effluents during rainstorms (Zhou et al., 2020). C1 and C3 can be categorized into protein-like components and likely linked to household and industrial wastewater inputs (Hosen et al., 2014; Zhou et al., 2022). When the water levels of the two rivers were lower than 3.8 m.a.s.l (flood warning water level of both rivers), the DOC concentrations and BDOC of the two rivers rose with increasing water levels associated with rainfall events (Fig. 2). This is likely due to the flushing of a large quantity of plant debris, household effluents, and terrestrial DOM caused by enhanced rainfall in the watershed (Dhillon and Inamdar 2013; Hosen et al., 2014). For example, Hosen et al. (2014) found that mobilization and input of fresh DOM with high bio-lability contributed markedly to elevated BDOC. In comparison, during rainstorms, when the water levels of the two rivers were higher than 3.8 m.a.s.l., i.e. above the flood warning water level of both rivers after long-term rainfall, we found that both DOC and BDOC decreased with increasing water levels in the two rivers (Fig. 2). The scatter found in the positive relationships between DOC and water level (Fig. 2) is likely due to a lag time between peak water levels and peak DOC exports. Decreased DOC with increasing water level in both rivers is consistent with a previous study finding that DOC decreased with inflowing discharge due to local dilution (Zhou et al., 2020) and a result of more water bypassing direct contact with soils and urban surfaces. The concentration of DOC peaked on the rising limb of flood discharge hydrographs and rapidly decreasing with continuation of rainstorm events is typical (Hood et al., 2006; Yoon and Raymond, 2012). The summed DOC and BDOC fluxes from the two rivers were up to 1.44 × $10^4$ t C yr$^{-1}$ and 0.28 × $10^4$ t C yr$^{-1}$, respectively, both being comparable with the summed inflowing DOC and BDOC fluxes to Lake Qiandao, one of the largest drinking water lakes in China with a watershed area of 1.04 × $10^4$ km$^2$ (Zhou et al., 2020). In total, more than 170 rivers or channels connect to Lake Taihu (Qin et al., 2007), implying that the summed annual inflowing fluxes of DOC and BDOC can be much higher than those from the two tributaries recorded in this study. DOC and BDOC decreased, while the amount of river water rose with increasing water level in both rivers during flood warning water level periods (Fig. 2), as also seen by Yang et al. (2019), and we found notably higher inflowing DOC and BDOC fluxes during rainstorms compared with the other seasons.

The molecular composition of DOM identified via FT-ICR MS revealed increased relative abundance of polycyclic and condensed aromatic and polyphenolic compounds coupled with decreased relative abundance of aliphatic compounds during rainstorms with high water levels (Fig. 7b), and this provides further evidence of the hypothesis that rainstorms enhanced the aromatic nature of DOM, despite being more bio-labile. The elevated $m/z$ during rainstorms with high water levels compared with low $m/z$ during the dry season with low water levels (Fig. 7) suggests the occurrence of a higher molecular weight of DOM during rainstorms compared with other time periods. Meanwhile, we found that the relative abundance of polycyclic and condensed aromatic and polyphenolic compounds increased with increasing water level, while the relative abundance of highly unsaturated and phenolic and aliphatic compounds decreased with increasing water level (Fig. 7c-f). The close positive linkages between aromatic formulae and %terrestrial humic-like C2 (Fig. 7c) highlight a consistency between the bulk optical and molecular-level composition of DOM, indicating that optical measurements coupled with ultrahigh-resolution mass spectrometry are promising tools to unravel the cycling of DOM.

Rainfall, especially rainstorms, controls the inflow discharge and thereby the water level of Lake Taihu located in a monsoon climate watershed, and our results indicate an increased frequency of heavy rainfall (≥ 25 mm d$^{-1}$) and rainstorm (≥ 50 mm d$^{-1}$) events and enhanced intensity of heavy rainfall events during the past six decades (Fig. 8). This implies that a higher frequency of elevated inputs of terrestrial soil and litter layer organic-rich DOM with high aromaticity from the upstream rivers to the lake is to be expected in a future wetter climate with more rainstorms in the watershed. Lakes are hotspots for the global carbon cycling and key sources of drinking water supply to large and mega cities globally. In Lake Taihu, riverine DOM derived from the inflowing rivers of the watershed contributes primarily to the DOM pool and thus controls the chemical composition and bio-lability of DOM in the lake. $SUVA_{254}$ has been used as an indicator of the removal

efficiency of DOM during water treatment (Kothawala et al., 2017), and we observed that rainstorm events enhanced the aromaticity of DOM discharged into the lake, implying a higher removal efficiency of DOM in a future wetter climate in the watershed. The inflowing lake regions typically the area at the intersection of both allochthonous and autochthonous DOM, they often have intense priming effects (Bianchi 2011) and exhibit various biogeochemical processes, and they are thus hotspots of greenhouse gas emissions. Rainstorm events will mobilize substantial freshly produced DOM as well as household effluents, soil organic matter, and organic debris from imperious landscapes in the upstream watersheds. These organic substances provide a large quantity of bio-labile organic carbon substrate for heterotrophic microbes in the lake, particularly in the inflowing lake areas. Future studies may be conducted to unravel the linkages between rainstorm events and greenhouse gas emissions in the inflowing lake areas, as well as drinking water treatability for lake systems with important ecosystem services such as Lake Taihu.

## 5. Conclusions

Using extensive and long-term high-frequency observations, we demonstrated how rainfall, particularly rainstorm events, shifts the molecular composition and bio-lability of DOM exported to Lake Taihu. Our results indicated that rainfall events enhanced the export of DOM with high aromaticity and bio-lability to the lake, while rainstorms resulted in diluted DOC and lower BDOC but elevated aromaticity. We estimated that the annual mean inflow fluxes of DOC to Lake Taihu were $1.15 \pm 0.14 \times 10^4$ t C $yr^{-1}$ from River Dapu and $2.92 \pm 0.38 \times 10^3$ t C $yr^{-1}$ from River Yincun and that the annual BDOC inflow fluxes were $0.23 \pm 0.06 \times 10^4$ t C $yr^{-1}$ from River Dapu and $0.53 \pm 0.07 \times 10^3$ t C $yr^{-1}$ from River Yincun. FT-ICR MS results showed an increased relative abundance of polycyclic and condensed aromatic and polyphenolic compounds and reduced relative abundance of the highly unsaturated and phenolic and aliphatic compounds during rainstorm events. Enhanced input of aromatic and concurrent bio-labile DOC to the lake is to be expected in a future wetter climate with increased occurrence of heavy rainfall and rainstorm events.

## Declaration of Competing Interest

The authors declare that they have no known competing financial interests or personal relationships that could have appeared to influence the work reported in this paper.

## Data availability

Data will be made available on request.

## Acknowledgments

This work was supported by the National Natural Science Foundation of China (grants 42207447, 41930760, 41977322, and 42071118), the Youth Innovation Promotion Association, CAS (2021312), NIGLAS Foundation (E1SL002, 2022NIGLAS-CJH04, and 2022SKL008), the Provincial Natural Science Foundation of Jiangsu (BK20220162 and BK20220041), and the Chinese Postdoctoral Science Foundation (BX2021325). EJ was supported by the TÜBITAK program BIDEB2232 (project 118C250). We thank Yu Shi, Liuqing Zhang, Yanni Guo, Yuyang Li, Huimin Chen, and Lili Chen for their help with field and laboratory measurements and Anne Mette Poulsen from Aarhus University for English editions. We thank Prof. Mark van Loosdrecht and the three anonymous reviewers for their helpful comments.

## Supplementary materials

Supplementary material associated with this article can be found, in the online version, at doi:10.1016/j.watres.2022.119448.

## References

Abbott, B.W., Larouche, J.R., Jones, J.B., Bowden, W.B., Balser, A.W., 2014. Elevated dissolved organic carbon biodegradability from thawing and collapsing permafrost. J. Geophys. Res. 119 (10), 2049–2063.
Baghoth, S.A., Sharma, S.K., Amy, G.L., 2011. Tracking natural organic matter (NOM) in a drinking water treatment plant using fluorescence excitation–emission matrices and PARAFAC. Water Res. 45 (2), 797–809.
Bianchi, T.S., 2011. The role of terrestrially derived organic carbon in the coastal ocean: A changing paradigm and the priming effect. Proc. Nat. Acad. Sci. U.S.A. 108 (49), 19473–19481.
Cédric, G.F., Benner, R., 2012. The spectral slope coefficient of chromophoric dissolved organic matter (S275-295) as a tracer of terrigenous dissolved organic carbon in river-influenced ocean margins. Limnol. Oceanogr. 57 (5), 1453–1466.
Choi, J., Jang, E., Yoon, Y.J., Park, J., Kim, T.W., Becagli, S., Caiazzo, L., Cappelletti, D., Krejci, R., Eleftheriadis, K., 2019. Influence of biogenic organics on the chemical composition of Arctic aerosols. Global Biogeochem. Cycles 33 (10), 1238–1250.
Coward, E.K., Ohno, T., Sparks, D.L., 2019. Direct evidence for temporal molecular fractionation of dissolved organic matter at the iron oxyhydroxide interface. Environ. Sci. Technol. 53 (2), 642–650.
Dhillon, G.S., Inamdar, S., 2013. Extreme storms and changes in particulate and dissolved organic carbon in runoff: entering uncharted waters? Geophys. Res. Lett. 40 (7), 1322–1327.
Dilling, J., Kaiser, K., 2002. Estimation of the hydrophobic fraction of dissolved organic matter in water samples using UV photometry. Water Res. 36 (20), 5037–5044.
Drake, T.W., Podgorski, D.C., Dinga, J.B., Chanton, J., Six, J., Spencer, R.G.M., 2019. Land-use controls on carbon biogeochemistry in lowland streams of the Congo Basin. Global Change Biol. 26 (3), 1374–1389.
Drake, T.W., Raymond, P.A., Spencer, R.G.M., 2018. Terrestrial carbon inputs to inland waters: a current synthesis of estimates and uncertainty. Limnol. Oceanogr Lett 3, 132–142.
Edzwald, J.K., Tobiason, J.E., 1999. Enhanced coagulation: US requirements and a broader view. Water Sci. Technol. 40 (9), 63–70.
Fasching, C., Ulseth, A.J., Schelker, J., Steniczka, G., Battin, T.J., 2016. Hydrology controls dissolved organic matter export and composition in an Alpine stream and its hyporheic zone. Limnol. Oceanogr. 61 (2), 558–571.
Fu, Q.-L., Fujii, M., Kwon, E., 2020. Development and application of a high-precision algorithm for nontarget identification of organohalogens based on ultrahigh-resolution mass spectrometry. Anal. Chem. 92 (20), 13989–13996.
Helms, J.R., Stubbins, A., Ritchie, J.E., Minor, E.C., Kieber, D.J., Mopper, K., 2008. Absorption spectral slopes and slope ratios as Indicators of molecular weight, source, and photobleaching of chromophoric dissolved organic matter. Limnol. Oceanogr. 53 (3), 955–969.
Hood, E., Gooseff, M.N., Johnson, S.L., 2006. Changes in the character of stream water dissolved organic carbon during flushing in three small watersheds. J. Geophys. Res. 111, G01007.
Hosen, J.D., McDonough, O.T., Febria, C.M., Palmer, M.A., 2014. Dissolved organic matter quality and bioavailability changes across an urbanization gradient in headwater streams. Environ. Sci. Technol. 48 (14), 7817–7824.
Huguet, A., Vacher, L., Relexans, S., Saubusse, S., Froidefond, J.-M., Parlanti, E., 2009. Properties of fluorescent dissolved organic matter in the Gironde Estuary. Org. Geochem. 40 (6), 706–719.
Hur, J., Lee, B.M., Lee, S., Shin, J.K., 2014. Characterization of chromophoric dissolved organic matter and trihalomethane formation potential in a recently constructed reservoir and the surrounding areas-Impoundment effects. J. Hydrol. 515 (16), 71–80.
Johnston, S.E., Striegl, R.G., Bogard, M.J., Dornblaser, M.M., Butman, D.E., Kellerman, A.M., Wickland, K.P., Podgorski, D.C., Spencer, R.G.M., 2020. Hydrologic connectivity determines dissolved organic matter biogeochemistry in northern high-latitude lakes. Limnol. Oceanogr. 65 (8), 1764–1780.
Jung, C.W., Son, H.J., 2008. The relationship between disinfection by-products formation and characteristics of natural organic matter in raw water. Korean J. Chem. Eng. 25 (4), 714–720.
Kellerman, A.M., Arellano, A., Podgorski, D.C., Martin, E.E., Martin, J.B., Deuerling, K.K., Bianchi, T.S., Spencer, R.G.M., 2019. Fundamental drivers of dissolved organic matter composition across an Arctic effective precipitation gradient. Limnol. Oceanogr. 65 (6), 1217–1234.
Kellerman, A.M., Kothawala, D.N., Dittmar, T., Tranvik, L.J., 2015. Persistence of dissolved organic matter in lakes related to its molecular characteristics. Nat. Geosci. 8 (6), 454–457.
Koch, B., Dittmar, T., 2016. From mass to structure: An aromaticity index for high-resolution mass data of natural organic matter. Rapid Commun. Mass Spectrom. 30 (1), 250. -250.
Koch, B.P., Dittmar, T., 2006. From mass to structure: an aromaticity index for high-resolution mass data of natural organic matter. Rapid Commun. Mass Spectrom. 20 (5), 926–932.
Kothawala, D.N., Köhler, S.J., Östlund, A., Wiberg, K., Ahrens, L., 2017. Influence of dissolved organic matter concentration and composition on the removal efficiency of

perfluoroalkyl substances (PFASs) during drinking water treatment. Water Res. 121, 320–328.
Kothawala, D.N., Stedmon, C.A., Muller, R.A., Weyhenmeyer, G.A., Kohler, S.J., Tranvik, L.J., 2014. Controls of dissolved organic matter quality: evidence from a large-scale boreal lake survey. Global Change Biol. 20 (4), 1101–1114.
Lynch, L.M., Sutfin, N.A., Fegel, T.S., Boot, C.M., Covino, T.P., Wallenstein, M.D., 2019. River channel connectivity shifts metabolite composition and dissolved organic matter chemistry. Nat. Commun. 10, 459.
Margaret, A.B., Holly, R.B., Rachel, S.G., Diane, M.M., Paul, D.B., 2016. Dissolved organic matter transport reflects hillslope to stream connectivity during snowmelt in a montane catchment. Water Resour. Res. 52 (6), 4905–4923.
Murphy, K.R., Hambly, A., Singh, S., Henderson, R.K., Baker, A., Stuetz, R., Khan, S.J., 2011. Organic matter fluorescence in municipal water recycling schemes: Toward a unified PARAFAC model. Environ. Sci. Technol. 45 (7), 2909–2916.
Murphy, K.R., Stedmon, C.A., Graeber, D., Bro, R., 2013. Fluorescence spectroscopy and multi-way techniques. PARAFAC. Anal. Methods 5 (23), 6557–6566.
Murphy, K.R., Stedmon, C.A., Wenig, P., Bro, R., 2014. OpenFluor–an online spectral library of auto-fluorescence by organic compounds in the environment. Anal. Methods 6 (3), 658–661.
Qin, B., Paerl, H.W., Brookes, J.D., Liu, J., Jeppesen, E., Zhu, G., Zhang, Y., Xu, H., Shi, K., Deng, J., 2019. Why Lake Taihu continues to be plagued with cyanobacterial blooms through 10 years (2007–2017) efforts. Sci. Bull. 64 (6), 354–356.
Qin, B., Xu, P., Wu, Q., Luo, L., Zhang, Y., 2007. Environmental issues of Lake Taihu. Hydrobiologia 581 (1), 3–14.
Raymond, P.A., Saiers, J.E., 2010. Event controlled DOC export from forested watersheds. Biogeochemistry 100 (1), 197–209.
Sankar, M.S., Dash, P., Singh, S., Lu, Y.H., Mercer, A.E., Chen, S., 2019. Effect of photo-biodegradation and biodegradation on the biogeochemical cycling of dissolved organic matter across diverse surface water bodies. J. Environ. Sci. 77, 130–147.
Spencer, R.G.M., Guo, W.D., Raymond, P.A., Dittmar, T., Hood, E., Fellman, J., Stubbins, A., 2014. Source and biolability of ancient dissolved organic matter in glacier and lake ecosystems on the Tibetan Plateau. Geochim. Cosmochim. Acta 142, 64–74.
Spencer, R.G.M., Hernes, P.J., Dinga, B., Wabakanghanzi, J.N., Drake, T.W., Six, J., 2016. Origins, seasonality, and fluxes of organic matter in the Congo River. Global Biogeochem. Cycles 30 (7), 1105–1121.
Stedmon, C.A., Markager, S., 2005. Tracing the production and degradation of autochthonous fractions of dissolved organic matter by fluorescence analysis. Limnol. Oceanogr. 50 (5), 1415–1426.
Stedmon, C.A., Sobecka, B.S., Hansen, R.B., Tallec, N.L., Waul, C.K., Arvin, E., 2011. A potential approach for monitoring drinking water quality from groundwater systems using organic matter fluorescence as an early warning for contamination events. Water Res. 45 (18), 6030–6038.
Tomlinson, A., Drikas, M., Brookes, J.D., 2016. The role of phytoplankton as pre-cursors for disinfection by-product formation upon chlorination. Water Res. 102, 229–240.
Vonk, J.E., Tank, S.E., Mann, P.J., Spencer, R.G.M., 2015. Biodegradability of dissolved organic carbon in permafrost soils and aquatic systems: a meta-analysis. Biogeosciences 23 (12), 6915–6930.
Walker, S.A., Amon, R.M.W., Stedmon, C.A., 2013. Variations in high-latitude riverine fluorescent dissolved organic matter: a comparison of large Arctic rivers. J. Geophys. Res. 118 (4), 1689–1702.
Weishaar, J.L., Aiken, G.R., Bergamaschi, B.A., Fram, M.S., Fujii, R., Mopper, K., 2003. Evaluation of specific ultravoilet absorbance as an indicator of the chemical composition of reactivity of dissolved organic matter. Environ. Sci. Technol. 37, 4702–4708.
Yamashita, Y., Boyer, E., Rudolf, J., 2013. Evaluating the distribution of terrestrial dissolved organic matter in a complex coastal ecosystem using fluorescence spectroscopy-ScienceDirect. Cont. Shelf Res. 66 (9), 136–144.
Yamashita, Y., Jaffé, R., 2008. Characterizing the interactions between trace metals and dissolved organic matter using excitation-emission matrix and parallel factor analysis. Environ. Sci. Technol. 42 (19), 7374–7379.
Yang, L., Chang, S.-W., Shin, H.-S., Hur, J., 2015. Tracking the evolution of stream DOM source during storm events using end member mixing analysis based on DOM quality. J. Hydrol. 523, 333–341.
Yang, L., Chen, W., Zhuang, W.E., Cheng, Q., Li, W., Wang, H., Guo, W., Chen, C.T.A., Liu, M., 2019. Characterization and bioavailability of rainwater dissolved organic matter at the southeast coast of China using absorption spectroscopy and fluorescence EEM-PARAFAC. Estuarine Coastal Shelf Science 217 (FEB.5), 45–55.
Yoon, B., Raymond, P.A., 2012. Dissolved organic matter export from a forested watershed during Hurricane Irene. Geophys. Res. Lett. 39 (18), L18402.
Zhang, Y.L., Gao, G., Shi, K., Niu, C., Zhou, Y.Q., Qin, B.Q., Liu, X.H., 2014. Absorption and fluorescence characteristics of rainwater CDOM and contribution to Lake Taihu. China. Atmosph. Environ. 98, 483–491.
Zhou, Y., Liu, M., Zhou, L., Jang, K.S., Xu, H., Shi, K., Zhu, G., Liu, M., Deng, J., Zhang, Y., Spencer, R.G.M., Kothawala, D.N., Jeppesen, E., Wu, F, 2020. Rainstorm events shift the molecular composition and export of dissolved organic matter in a large drinking water reservoir in China: High frequency buoys and field observations. Water Res. 187, 116471.
Zhou, Y., Xiao, Q., Yao, X., Zhang, Y., Zhang, M., Shi, K., Lee, X., Podgorski, D.C., Qin, B., Spencer, R.G.M., Jeppesen, E., 2018a. Accumulation of terrestrial dissolved organic matter potentially enhances dissolved methane levels in eutrophic Lake Taihu, China. Environ. Sci. Technol. 52 (18), 10297–10306.
Zhou, Y., Yao, X., Zhang, Y., Shi, K., Zhang, Y., Jeppesen, E., Gao, G., Zhu, G., Qin, B., 2017. Potential rainfall-intensity and pH-driven shifts in the apparent fluorescent composition of dissolved organic matter in rainwater. Environ. Pollut. 224, 638–648.
Zhou, Y., Yao, X., Zhang, Y., Zhang, Y., Shi, K., Tang, X., Qin, B., Podgorski, D.C., Brookes, J.D., Jeppesen, E., 2018b. Response of dissolved organic matter optical properties to net inflow runoff in a large fluvial plain lake and the connecting channels. Sci. Total Environ. 639, 876–887.
Zhou, Y., Zhou, L., Zhang, Y., Zhu, G., Qin, B., Jang, K.S., Spencer, R.G.M., Kothawala, D. N., Jeppesen, E., Brookes, J.D., Wu, F., 2022. Unraveling the role of anthropogenic and natural drivers in shaping the molecular composition and biolability of dissolved organic matter in non-pristine lakes. Environ. Sci. Technol. 56 (7), 4655–4664.